Helical chiral N-heterocyclic carbene ligands in enantioselective gold catalysis

Lenka Pallova, Laura Abella, Marion Jean, Nicolas Vanthuyne, Cécile Barthes, Laure Vendier, Jochen Autschbach, Jeanne Crassous, Stéphanie Bastin, Vincent César

Helical chiral N-heterocyclic carbene ligands in enantioselective gold catalysis

Lenka Pallova,[a] Laura Abella,[d] Marion Jean,[c] Nicolas Vanthuyne,[c] Cécile Barthes,[a] Laure Vendier,[a] Jochen Autschbach,*[d] Jeanne Crassous,*[b] Stéphanie Bastin,*[a] Vincent César*[a]

[a] Dr. L. Pallova, C. Barthes, Dr. L. Vendier, Dr. S. Bastin, Dr. V. César
LCC-CNRS
Université de Toulouse, CNRS, Toulouse, France
E-mail: stephanie.bastin@lcc-toulouse.fr
vincent.cesar@lcc-toulouse.fr

[b] Dr. J. Crassous
Institut des Sciences Chimiques de Rennes, UMR 6226
Institut de Physique de Rennes, UMR 6251, Campus de Beaulieu
CNRS-Université de Rennes 1, 35042 Rennes Cedex (France)
E-mail: jeanne.crassous@univ-rennes1.fr

[c] M. Jean, Dr. N. Vanthuyne
Aix Marseille university, CNRS, Centrale Marseille, Ism2
Marseille (France)

[d] Dr. L. Abella, Prof. J. Autschbach
Department of chemistry
University at Buffalo – State University of New York
Buffalo, NY 14260 (USA)
E-mail: jochena@buffalo.edu

Supporting information for this article is given via a link at the end of the document.

Abstract: The first chiral helicene-NHC gold(I) complexes efficient in enantioselective catalysis were prepared. The L-shaped chiral ligand is composed of an imidazo[1,5-*a*]pyridin-3-ylidene (IPy) scaffold laterally-substituted by a configurationally stable [5]-helicenoid unit. The chiral information was introduced in a key post-functionalization step of a NHC-gold(I) complex bearing a symmetrical anionic fluoreno[5]helicene substituent, leading to a racemic mixture of complexes featuring three correlated elements of chirality, namely central, axial and helical chirality. After HPLC enantiomeric resolution, X-ray crystallography and theoretical calculations enabled structural and stereochemical characterization of these configurationally stable NHC-gold(I) complexes. The high potential in asymmetric catalysis is demonstrated in the benchmark cycloisomerization of N-tethered 1,6-enynes with up to 95:5 er.

Introduction

Helicenes and helicene-like compounds, composed of o*rtho*-annelated polycyclic skeletons, are inherently chiral molecules, which feature a helical topology due to geometrical constraints.[1] Their screw-shape π-extended electronic structure confers them unique enhanced chiroptical properties,[1,2] leading to continually emerging applications in material science such as in optoelectronic materials,[3] supramolecular chemistry,[4] or spin-based devices.[5] Owing to the extended chiral 3D structures, helicenes were also successfully applied as key constitutional chiral units in asymmetric organic and transition metal catalysis, leading to some efficient chiral helical N- and P-based ligands.[6]

The first chiral helicenic N-Heterocyclic Carbene (NHC) complex was prepared in 2016 [7] by combining a chiral helicenic moiety within the powerful NHC ligands.[8,9] This opened the way to significant developments mainly focused on chiral helicenic NHC-complexes with intriguing emission properties.[10] However, to our knowledge, only two chiral helicenic NHC-systems have so far been implemented in asymmetric catalysis, and the research area is still in its infancy.[11] In particular, the key design principles for an efficient chiral induction remain to be determined.[12]

Ligand design is especially important in asymmetric gold(I) catalysis due to the linear geometry of Au(I) complexes, which brings the incoming substrate in *trans* position relative to the stereoinducting ligand and requires the construction of an extended 3D chiral pocket embedding the distal active site.[13] A relevant example was reported by Voituriez, Marinetti and coll. who developed efficient chiral phosphahelicene-gold systems with the Au(I) center positioned in the inner rim of the helicenic phosphine ligand.[14] Applying this design principle to NHC ligands, we set out to have now a chiral helicenic-NHC ligand, in which a configurationally stable pentahelicenic moiety is grafted at the position 5 of the imidazo[1,5-*a*]pyridin-3-ylidene scaffold (Figure 1).

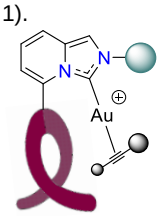

- L-shape, chiral helical NHC ligand
- Au(I) center in the groove of the helix
- Chiral information close to the incoming alkyne
- Possibility of steric tuning

Figure 1. Targeted helical NHC Au(I) catalysts placing the chiral helicene-like moiety near the cationic gold center and the incoming alkyne substrate.

The latter N-heterobicyclic carbene platform has already been shown to generate powerful (axially chiral) NHC ligands for gold(I) catalysis; its specific geometry would bring the lateral chiral helicenic group closer to the gold(I) center and to the active site.[15-17]

Results and Discussion

We recently reported an efficient functionalization of the imidazo[1,5-*a*]pyridinium scaffold based on a late-stage aromatic nucleophilic substitution strategy starting from 5-bromoimidazo[1,5-*a*]pyridinium bromide **1** (Scheme 1).[15,18] This prompted us to select fluorenyl-derived [*n*]helicenes (n = 5 or 7)[19] as potential helical candidates and nucleophiles and we started our investigations with the achiral dibenzo[*c,g*]fluorene **2** (Scheme 1).

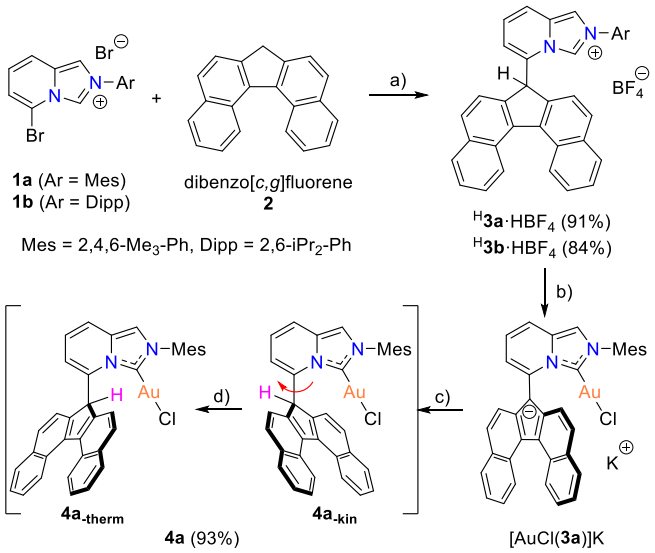

Scheme 1. Synthesis of the achiral imidazolium salts **3a-b**·HBF_4 and of gold(I) complex **4a**. Reagents and conditions: a) *i*) **2**, NaH (2.0 equiv), DMF, RT, 25 min; *ii*) **1a-b** (1.0 equiv), RT, 1.5 h; *iii*) HBF_4 (3 equiv); b) *i*) KHMDS (2.0 equiv), THF, - 50°C; *ii*) AuCl(tht) (1.0 equiv), -50°C, 1h; c) HCl, THF, -50°C; d) $CDCl_3$, 25°C.

The fluorenide-type anion derived from **2** (generated by deprotonation with NaH) rapidly and cleanly displaced the bromide substituent in **1a-b** at room temperature to afford the corresponding imidazo[1,5-*a*]pyridinium salts ^{H}**3a-b**·HBF_4 after a last step of reprotonation in good to excellent yields and on gram scale. The air- and water-stable salts ^{H}**3a-b**·HBF_4 were fully characterized and their formulation was confirmed by X-Ray diffraction on single crystals of the mesityl derivative ^{H}**3a**·HBF_4 (Figure 2a).[20]

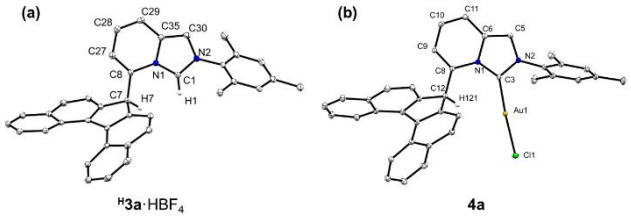

Figure 2. Molecular structures of (a) ^{H}**3a**·HBF_4 (left) and (b) **4a** (right) (ellipsoids drawn at 30% probability level). BF_4^- anion and hydrogen atoms (except on the apical 'fluorenyl' position and on the pre-carbenic position) have been omitted for clarity. Selected bond lengths (Å) and angles (deg) for **4a**: Au1-C3 1.985(3), Au1-H121 2.634, C3-Au1-Cl1 175.04(7), Au1-C3-N1 134.52(19), Au1-C3-N2 121.61(18).

The potassium salt of the anionic free NHC [**3a**](K) was generated by deprotonation of ^{H}**3a**·HBF_4 using two equivalents of potassium bis(trimethylsilyl)amide (KHMDS) and the carbene center was trapped by AuCl(tht) at -50°C to give *in situ* the corresponding anionic gold(I) complexes [AuCl(**3a**)](K). After a final reprotonation step of the lateral fluorenyl-type moiety, neutral complex **4a** was isolated in an excellent 93% overall yield. Interestingly, we observed a complete and irreversible conversion of the kinetic product **4a**$_{\text{-kin}}$ into the more stable thermodynamic product **4a**$_{\text{-therm}}$. The formulation of these conformers was inferred in particular from the high-field shift of the *ortho*-methyl protons of the mesityl group in **4a**$_{\text{-kin}}$ (δ = 1.54 ppm) and from the strong deshielding of the fluorenyl-type proton of the helicenic moiety from δ = 5.11 ppm in **4a**$_{\text{-kin}}$ to δ = 8.39 ppm in **4a**$_{\text{-therm}}$ (see supporting information for details). The formation of the kinetic conformer **4a**$_{\text{-kin}}$ is thus proposed to proceed through an outer-sphere protonation of the anionic intermediate [AuCl(**3a**)]K, pushing the helicenic moiety towards the inner coordination sphere. This steric crowding is then released by rotation around the C-C bond between the IPy and helicenic moieties leading to **4a**$_{\text{-therm}}$, in which the helicenic unit is oriented in the opposite direction relative to the gold center and, conversely, the fluorenyl-type CH bond points towards the gold center. This conformation was confirmed by an X-Ray diffraction analysis (Figure 2b). Noteworthy the relatively short Au1-H121 distance of 2.634 Å would suggest a weak "contra-electrostatic H bond", which would account for the strong proton chemical shift change $\Delta\delta$ = 3.28 ppm of the fluorenyl proton from **4a**$_{\text{-kin}}$ to **4a**$_{\text{-therm}}$.[21] Additionally, while not configurationally-stable in solution, the lateral fluoreno[5]helicene moiety featured an helicity (dihedral angle between the terminal rings) of 38.03° in the crystal structure. Complex **4a** was further evaluated as pre-catalyst in the model reaction of the gold-catalyzed cycloisomerization of N-tethered 1,6-enynes but was shown to rapidly decompose. Assuming that this low activity is due to presence of the quite acidic fluorenyl proton which might interfere in the catalytic cycle, we thus devised to replace this proton by an alkyl group by alkylation of intermediate [AuCl(**3a**)]K.

Hence, a small excess of benzyl bromide was added to the anionic intermediate complexes [AuCl(**3a-b**)]K in DMF, which led to a complete and very clean conversion after stirring overnight at room temperature (Scheme 2). Surprisingly, while the benzylation of the ligands **3a-b** was proven by mass spectrometry, the ^{1}H NMR spectra were not consistent with a benzylation at the "apical" fluorenyl position C_a. A total loss of symmetry was indeed observed and most importantly the benzylic CH_2 protons became

diastereotopic, giving two doublets around 3.5 ppm and 4.0 ppm in ^{1}H NMR spectrum. This indicated that the complexes became chiral during this step. The molecular structures of **5a-b** were then firmly established by XRD analysis of single crystals of **5a**. Complex **5a** crystallizes in the centrosymmetric space group P21/c and consists of a racemate; the two enantiomers are depicted in Figure 3. The benzylation reaction occurred on the positions C_b and C_c located in the inner rim of the dibenzofluorene moiety, which are the allylic counterparts of the non-accessible C_a position. Following an outer-sphere mechanism, the post-complexation functionalization thus created three types of chirality: *i*) a central chirality by the generation of the asymmetric sp^3 carbon atom C24 (Figure 3), *ii*) an axial chirality around the axis C7-C17, and *iii*) a helical chirality characterized by a helicity (dihedral angle between the terminal rings) of 53.74°. Interestingly, the HPLC analysis of **5a-b** on a chiral stationary phase confirmed that **5a-b** are racemic mixtures and the presence of only two peaks confirmed that the three chiralities are controlled even in solution. Chiral resolution on a preparative scale enabled their isolation in good yields and with high ee's (95% and 96% for (*R*,*Ra*,*M*)-**5a** and (*S*,*Sa*,*P*)-**5a**, respectively) and > 99% for (*R*,*Ra*,*M*)-**5b** and (*S*,*Sa*,*P*)-**5b**).[22] The absolute configuration was determined by comparing the experimental and calculated electronic circular dichroism (ECD) spectra (see supporting information for details) and confirmed by XRD analysis of a single crystal of the first eluted enantiomer of **5a** which appeared to be (*S*,*Sa*,*P*)-**5a**.

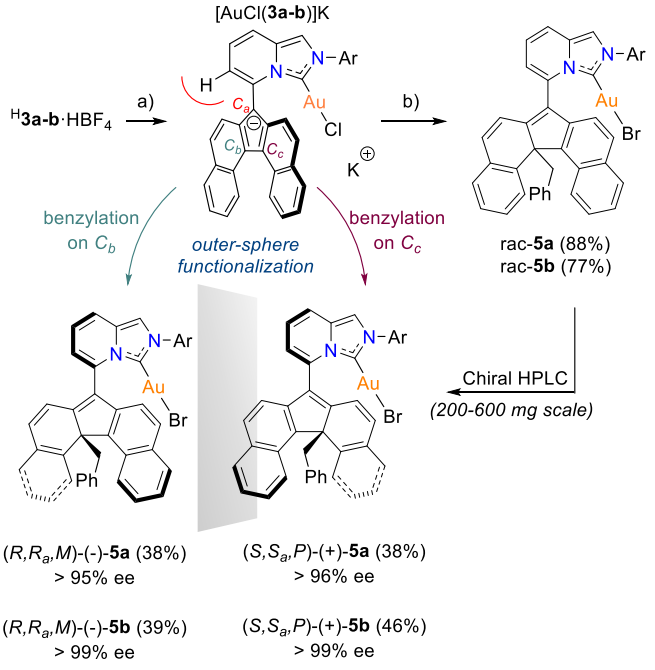

Scheme 2. Synthesis of optically pure gold(I) complexes **5a-b** through post-complexation functionalization. Reagents and conditions: a) *i*) KHMDS (2.0 equiv), THF, - 50°C; *ii*) AuCl(tht) (1.0 equiv), -50°C, 1h; b) BnBr (1.1 equiv), DMF, RT, 16-18h.

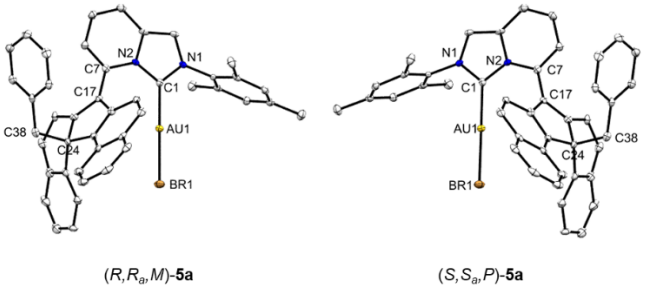

Figure 3. Molecular structures of the two enantiomers (*R*,*Ra*,*M*)-**5a** and (*S*,*Sa*,*P*)-**5a** crystallizing as a racemate (ellipsoids drawn at 30% probability level). Selected bond lengths (Å) and angles (deg): Au1-C1 1.983(5), C7-C17 1.469(7), C24-C38 1.590(7), C1-Au1-Br1 178.83(15).

Having the enantiopure helicenic NHC-gold(I) catalysts **5a-b** available, we proceeded to their evaluation in asymmetric catalysis by investigating the benchmark cycloisomerization of the N-tethered 1,6-enynes **6** into the bicyclo[4.1.0]heptene **7**,[14a,23-24]. Optimization of the reaction conditions was carried out with the model substrate **6a** (Table 1).

Table 1. Optimization of the reaction conditions for the cycloisomerization of N-tethered 1,6-enyne **6a**.[a]

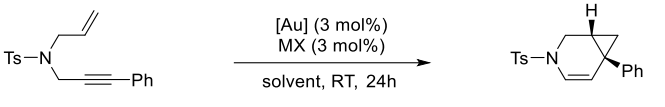

6a **7a**

Entry	[Au]	MX	solvent	Conv (%)[b]	yield (%)[b]	er[c]
1	(-)-**5a**	$AgNTf_2$	CH_2Cl_2	49	44	81:19
2	(-)-**5b**	$AgNTf_2$	CH_2Cl_2	94	55	71:29
3	(-)-**5a**	$AgNTf_2$	Et_2O	49	43	88:12
4	(-)-**5a**	$AgNTf_2$	toluene	56	55	92:8
5	(-)-**5a**	$AgNTf_2$	PhCl	68	65	92:8
6	(-)-**5a**	$NaBAr^F{}_4$[d]	PhCl	16	14	87:13
7	(-)-**5a**	$AgSbF_6$	PhCl	52	51	93:7
8	(-)-**5a**	AgOTf	PhCl	69	62	94:6
9	(+)-**5a**	AgOTf	PhCl	73	56	6.5:93.5
10[e]	(-)-**5a**	AgOTf	PhCl	46	46	95.5:4.5

[a] All reactions were carried out on a 0.1 mmol scale and at 0.1 M in substrate. [b] Determined by ^{1}H NMR using ferrocene as an internal standard. [c] Determined by HPLC analysis with a chiral stationary phase. [d] 6 mol%. [e] at 0°C for 72 h.

Gratifyingly, upon activation with $AgNTf_2$ in CH_2Cl_2, both pre-catalysts (*R*,*Ra*,*M*)-(-)-**5a** and (*R*,*Ra*,*M*)-(-)-**5b** gave satisfactory conversions and yields and more importantly promising stereoselectivities of 81:19 and 71:29 in product **7a** respectively (Table 1, entries 1-2). It appeared here that the outcome of the catalysis is influenced by the steric hindrance of the N-aryl group of the chiral NHC ligand, with mesityl group in (*R*,*Ra*,*M*)-(-)-**5a**

giving better results than the bulkier 2,6(diisopropyl)phenyl group in (*R,R*$_a$,*M*)-(-)-**5b**. Using the most stereoinducting pre-catalyst (*R,R*$_a$,*M*)-(-)-**5a**, we next investigated the influence of different solvents onto the selectivity of the reaction (Entries 3-5) and chlorobenzene was found to give both the best yields and enantiomeric ratios (65% yield, 92:8 er). Further screening of the pre-catalyst activator showed that the use of silver salt is required for activity as $NaBAr^F_4$ only gave very sluggish reaction and low yield (Entry 6). Among the silver salts (Entries 5,7,8), AgOTf appeared optimal in terms of yield and enantioselectivity (94:6 er). As expected, the opposite (*S,S*$_a$,*P*)-(+)-**5a** enantiomer led to similar results but with an inversed stereoselectivity and decreasing the reaction temperature to 0°C allowed an increased to 95.5:4.5 er but at the expense of a longer reaction time and lower yield.

With the optimized reaction conditions, the scope of the enantioselective cycloisomerization was evaluated (Scheme 3). Gratifyingly, the 1,6-enynes **6a-e** having different para-substituted aryl groups underwent cycloisomerization smoothly and gave the corresponding bicycles **7a-e** in almost constant enantiomeric ratios ranging from 93:7 for **7c** to 94.5:4.5 for **7d**, irrespective of the electron-withdrawing or donating character of the para-substituent. However, it appeared that the yield is more sensitive as a small yield erosion was observed for compounds **7e** and **7c** bearing a fluoride and a nitro substituent respectively. Moreover, a bulkier 1-naphthyl substituent on the alkyne moiety of **6f** was found compatible with the catalytic system and product **7f** was obtained in 67% yield and an excellent 94:6 er. Overall, the present system was shown quite versatile and efficient on this substrate scope and compared favorably with literature precedents. The latter included the phospha(thia)helicenes/Au(I) complexes with er between 84:16 and 93:7,[14a,25] and a bimetallic MeOBIPHEP(AuCl)$_2$ pre-catalyst, which gave very high enantioinduction for **7a** (99:1 er) but very low yields and much lower enantiomeric ratios for **7c** and **7d**.[26]

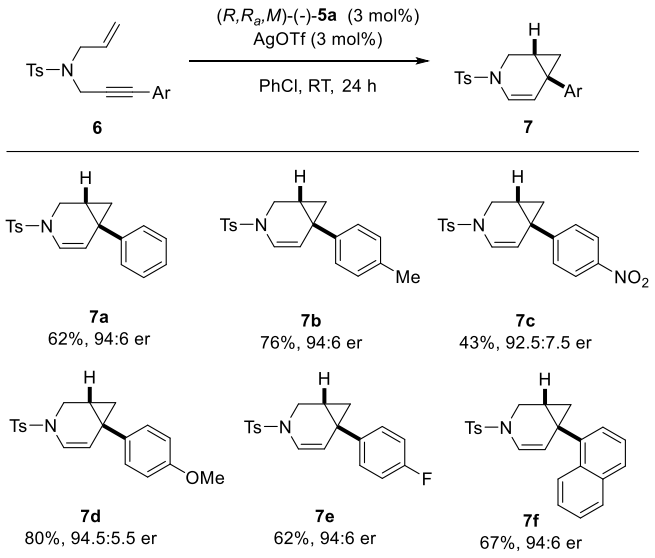

Scheme 3. Substrate scope of the cycloisomerization of N-tethered 1,6-enynes **6** catalyzed by (*R,R*$_a$,*M*)-(-)-**5a**. All reactions were conducted on a 0.1 mmol scale and in chlorobenzene (0.1 M). NMR yields on isolated product using ferrocene as internal standard. Enantiomeric ratio determined by analytical chiral HPLC.

Conclusion

In summary, we developed a new class of chiral, enantiopure helical NHC-gold complexes through an efficient and straightforward synthetic sequence. The key post-functionalization step created a new type of [5]-helicenoid unit, which is configurationally stable thanks to the presence of the asymmetric C(sp^3) carbon inside its inner groove. The stereoinducing potential of the enantiopure helical NHC-gold pre-catalysts was demonstrated in the benchmark Au(I)-catalyzed cycloisomerization of 1,6-enynes. This example demonstrates for the first time the efficiency of chiral NHC-Au(I) ligands bearing a substituted pentahelicenic unit[27] in enantioselective catalysis, thanks to a rational ligand design which forces the metal center to be directed toward the helical groove of the lateral substituent.[14] Extension of this methodology to the design of chiral helicenic NHC-complexes having longer and/or other types of fluorenyl-derived helicenoid moieties as well as the application of these chiral NHC systems in other asymmetric transformations are currently underway in our laboratories.

Acknowledgements

This work was supported by the Agence Nationale de la Recherche (ANR-16-CE07-0019 “Hel-NHC” grant) and the Centre National de la Recherche Scientifique (CNRS). L.A. and J.A. acknowledge the Center for Computational Research (CCR) at the University at Buffalo for providing computational resources.[28] The computational part of this research has been supported by Grant CHE-1855470 from the National Science Foundation.

Keywords: helicenes • N-heterocyclic carbenes • gold • asymmetric catalysis • chirality

[1] a) C.-F. Chen, Y. Shen, In Helicene Chemistry: From Synthesis to Applications, Springer, Berlin, Heidelberg, **2017**; b) K. Dhbaibi, L. Favereau, J. Crassous, *Chem. Rev.* **2019**, *119*, 8846-8953; c) M. Gingras, *Chem. Soc. Rev.* **2013**, *42*, 1051-1095; d) Y. Shen, C.-F. Chen, *Chem. Rev.* **2012**, *112*, 1463-1535.

[2] a) T. Mori, *Chem. Rev.* **2021**, *121*, 2373-2412; b) W.-L. Zhao, M. Li, H.-Y. Lu, C.-F. Chen, *Chem. Commun.* **2019**, *55*, 13793-13803.

[3] a) D.-W. Zhang, M. Li, C.-F. Chen, *Chem. Soc. Rev.* **2020**, *49*, 1331-1343; b) J. R. Brandt, F. Salerno, M. J. Fuchter, *Nat. Rev. Chem.* **2017**, *1*, 0045.

[4] Selected examples: a) E. S. Gauthier, R. Rodríguez, J. Crassous, *Angew. Chem. Int. Ed.* **2020**, *59*, 22840-22856; *Angew. Chem.* **2020**, *132*, 23036-23052; b) M. Roy, V. Berezhnaia, M. Villa, N. Vanthuyne, M. Giorgi, J.-V. Naubron, S. Poyer, V. Monnier, L. Charles, Y. Carissan, D. Hagebaum-Reignier, J. Rodriguez, M. Gingras, Y. Coquerel, *Angew. Chem. Int. Ed.* **2020**, *59*, 3264-3271; *Angew. Chem.* **2020**, *132*, 3290-3297 c) K. Nakano, H. Oyama, Y. Nishimura, S. Nakasako, K. Nozaki, *Angew. Chem. Int. Ed.* **2012**, *51*, 695-699; *Angew. Chem.* **2012**, *124*, 719-723; d) M. A. Shcherbina, X. Zeng, T. Tadjiev, G. Ungar, S. H. Eichhorn, K. E. S. Phillips, T. J. Katz, *Angew. Chem. Int. Ed.* **2009**, *48*, 7837-7840; *Angew. Chem.* **2009**, *121*, 7977-7980.

[5] V. Kiran, S. P. Mathew, S. R. Cohen, I. Hernandez Delgado, J. Lacour, R. Naaman, *Adv. Mater*. **2016**, *28*, 1957-1962.

[6] For reviews, see: a) C. S. Demmer, A. Voituriez, A. Marinetti, *C. R. Chimie* **2017**, *20*, 860-879; b) P. Aillard, A. Voituriez, A. Marinetti, *Dalton Trans.* **2014**, *43*, 15263-15278; c) M. J. Narcis, N. Takenaka, *Eur. J. Org. Chem.* **2014**, *2014*, 21-34.

[7] N. Hellou, C. Jahier-Diallo, O. Basle, M. Srebro-Hooper, L. Toupet, T. Roisnel, E. Caytan, C. Roussel, N. Vanthuyne, J. Autschbach, M. Mauduit, J. Crassous, *Chem. Commun.* **2016**, *52*, 9243-9246.

[8] For an overview, see: M. N. Hopkinson, C. Richter, M. Schedler, F. Glorius, *Nature* **2014**, *510*, 485-496.

[9] Selected recent reviews: a) Q. Zhao, G. Meng, S. P. Nolan, M. Szostak, *Chem. Rev.* **2020**, *120*, 1981-2048; b) C. Romain, S. Bellemin-Laponnaz, S. Dagorne, *Coord. Chem. Rev.* **2020**, *422*, 213411; c) E. Peris, *Chem. Rev.* **2018**, *118*, 9988-10031; d) V. Nesterov, D. Reiter, P. Bag, P. Frisch, R. Holzner, A. Porzelt, S. Inoue, *Chem. Rev.* **2018**, *118*, 9678-9842.

[10] a) N. Hellou, M. Srebro-Hooper, L. Favereau, F. Zinna, E. Caytan, L. Toupet, V. Dorcet, M. Jean, N. Vanthuyne, J. A. G. Williams, L. Di Bari, J. Autschbach, J. Crassous, *Angew. Chem. Int. Ed.* **2017**, *56*, 8236-8239; *Angew. Chem.* **2017**, *129*, 8348-8351; b) E. S. Gauthier, L. Abella, N. Hellou, B. Darquié, E. Caytan, T. Roisnel, N. Vanthuyne, L. Favereau, M. Srebro-Hooper, J. A. G. Williams, J. Autschbach, J. Crassous, *Angew. Chem. Int. Ed.* **2020**, *59*, 8394-8400; *Angew. Chem.* **2020**, *132*, 8472-8478; c) R. Tarrieu, I. H. Delgado, F. Zinna, V. Dorcet, S. Colombel-Rouen, C. Crévisy, O. Baslé, J. Bosson, J. Lacour, *Chem. Commun.* **2021**, *57*, 3793-3796; d) E. S. Gauthier, N. Hellou, E. Caytan, S. Del Fré, V. Dorcet, N. Vanthuyne, L. Favereau, M. Srebro-Hooper, J. A. G. Williams, J. Crassous, *Inorg. Chem. Front.* **2021**, *8*, 3916-3925; e) E. S. Gauthier, M. Cordier, V. Dorcet, N. Vanthuyne, L. Favereau, J. A. G. Williams, J. Crassous, *Eur. J. Org. Chem.* **2021**, 4767-4767.

[11] a) I. G. Sanchez, M. Samal, J. Nejedly, M. Karras, J. Klivar, J. Rybacek, M. Budesinsky, L. Bednarova, B. Seidlerova, I. G. Stara, I. Stary, *Chem. Commun.* **2017**, *53*, 4370-4373; b) M. Karras, M. Dąbrowski, R. Pohl, J. Rybáček, J. Vacek, L. Bednárová, K. Grela, I. Starý, I. G. Stará, B. Schmidt, *Chem. Eur. J.* **2018**, *24*, 10994-10998.

[12] Reviews on chiral NHCs: a) V. César, C. Fliedel, A. Labande, in "Chiral Ligands: Evolution of Ligand Libraries for Asymmetric Catalysis"(Editor: M. Dieguez), Taylor & Francis, **2021**, 195-231; b) M. Michalak, W. Kośnik, *Catalysts* **2019**, *9*, 890; c) D. Janssen-Muller, C. Schlepphorst, F. Glorius, *Chem. Soc. Rev.* **2017**, *46*, 4845-4854.

[13] a) R. P. Herrera, M. C. Gimeno, *Chem. Rev.* **2021**, *121*, 8311-8363; b) Y. Li, W. Li, J. Zhang, *Chem. Eur. J.* **2017**, *23*, 467-512; c) . Zi, F. Dean Toste, *Chem. Soc. Rev.* **2016**, *45*, 4567-4589.

[14] a) K. Yavari, P. Aillard, Y. Zhang, F. Nuter, P. Retailleau, A. Voituriez, A. Marinetti, *Angew. Chem. Int. Ed.* **2014**, *53*, 861-865; *Angew. Chem.* **2014**, *126*, 880-884; b) P. Aillard, D. Dova, V. Magne, P. Retailleau, S. Cauteruccio, E. Licandro, A. Voituriez, A. Marinetti, *Chem. Commun.* **2016**, *52*, 10984-10987; c) V. Magné, Y. Sanogo, C. S. Demmer, P. Retailleau, A. Marinetti, X. Guinchard, A. Voituriez, *ACS Catal.* **2020**, *10*, 8141-8148.

[15] Y. Tang, I. Benaissa, M. Huynh, L. Vendier, N. Lugan, S. Bastin, P. Belmont, V. César, V. Michelet, *Angew. Chem. Int. Ed.* **2019**, *58*, 7977-7981; *Angew. Chem.* **2019**, *131*, 8061-8065.

[16] a) J. Francos, F. Grande-Carmona, H. Faustino, J. Iglesias-Sigüenza, E. Díez, I. Alonso, R. Fernández, J. M. Lassaletta, F. López, J. L. Mascareñas, *J. Am. Chem. Soc.* **2012**, *134*, 14322-14325; b) J.-Q. Zhang, Y. Liu, X.-W. Wang, L. Zhang, *Organometallics* **2019**, *38*, 3931-3938.

[17] Reviews on annelated NHCs: a) N. U. D. Reshi, J. K. Bera, *Coord. Chem. Rev.* **2020**, *422*, 213334; b) J. Iglesias-Siguenza, C. Izquierdo, E. Diez, R. Fernandez, J. M. Lassaletta, *Dalton Trans.* **2016**, *45*, 10113-10117.

[18] a) I. Benaissa, L. Pallova, M.-E. Morantin, T. Lafitte, M. Huynh, C. Barthes, L. Vendier, N. Lugan, S. Bastin, V. César, *Chem. Eur. J.* **2019**, *25*, 13030-13036; b) K. Azouzi, C. Duhayon, I. Benaissa, N. Lugan, Y. Canac, S. Bastin, V. César, *Organometallics* **2018**, *37*, 4726-4735.

[19] L. Pallova, E. S. Gauthier, L. Abella, M. Jean, N. Vanthuyne, V. Dorcet, L. Vendier, J. Autschbach, J. Crassous, S. Bastin, V. César, *Chem. Eur. J.* **2021**, *27*, 7722–7730.

[20] Deposition Numbers 2115287 (for **^{H}3a-b**·HBF_4), 2115288 (for **4a**), 2115286 (for rac-**5a**), 2115289 (for (*S,Sa,P*)-**5a**) contain the supplementary crystallographic data for this paper. These data are provided free of charge by the joint Cambridge Crystallographic Data Centre and Fachinformationszentrum Karlsruhe.

[21] For recent and leading examples of C-H…Au interaction, please see: a) H. Darmandeh, J. Löffler, N. V. Tzouras, B. Dereli, T. Scherpf, K.-S. Feichtner, S. Vanden Broeck, K. Van Hecke, M. Saab, C. S. J. Cazin, L. Cavallo, S. P. Nolan, V. H. Gessner, *Angew. Chem. Int. Ed.* **2021**, *60*, 21014-21024; *Angew. Chem.* **2021**, *133*, 21182-21192; b) G. dos Passos Gomes, G. Xu, X. Zhu, L.-M. Chamoreau, Y. Zhang, O. Bistri-Aslanoff, S. Roland, I. V. Alabugin, M. Sollogoub, *Chem. Eur. J.* **2021**, *27*, 8127-8142.

[22] For a leading reference in the separation of racemic NHC-metal complexes, please see: L. Kong, J. Morvan, D. Pichon, M. Jean, M. Albalat, T. Vives, S. Colombel-Rouen, M. Giorgi, V. Dorcet, T. Roisnel, C. Crévisy, D. Nuel, P. Nava, S. Humbel, N. Vanthuyne, M. Mauduit, H. Clavier, *J. Am. Chem. Soc.* **2020**, *142*, 93-98.

[23] For a review, please see: M. Mato, A. Franchino, C. García-Morales, A. M. Echavarren, *Chem. Rev.* **2021**, *121*, 8613-8684.

[24] Selected examples: a) G. Zuccarello, J. G. Mayans, I. Escofet, D. Scharnagel, M. S. Kirillova, A. H. Pérez-Jimeno, P. Calleja, J. R. Boothe, A. M. Echavarren, *J. Am. Chem. Soc.* **2019**, *141*, 11858-11863; b) Z. Wu, K. Isaac, P. Retailleau, J.-F. Betzer, A. Voituriez, A. Marinetti, *Chem. Eur. J.* **2016**, *22*, 3278-3281; c) M. Guitet, P. Zhang, F. Marcelo, C. Tugny, J. Jiménez-Barbero, O. Buriez, C. Amatore, V. Mouriès-Mansuy, J.-P. Goddard, L. Fensterbank, Y. Zhang, S. Roland, M. Ménand, M. Sollogoub, *Angew. Chem. Int. Ed.* **2013**, *52*, 7213-7218; *Angew. Chem.* **2013**, *125*, 7354-7359; d) H. Teller, M. Corbet, L. Mantilli, G. Gopakumar, R. Goddard, W. Thiel, A. Fürstner, *J. Am. Chem. Soc.* **2012**, *134*, 15331-15342; e) A. Pradal, C.-M. Chao, P. Y. Toullec, V. Michelet, *Beilstein J. Org. Chem.* **2011**, *7*, 1021-1029; f) C.-M. Chao, D. Beltrami, P. Y. Toullec, V. Michelet, *Chem. Commun.* **2009**, 6988-6990.

[25] P. Aillard, A. Voituriez, D. Dova, S. Cauteruccio, E. Licandro, A. Marinetti, *Chem. Eur. J.* **2014**, *20*, 12373-12376.

[26] A. Pradal, C.-M. Chao, P. Y. Toullec, V. Michelet, *Beilstein J. Org. Chem.* **2011**, *7*, 1021-1029.

[27] Efficient pentahelicene-phosphine ligand in asymmetric Pd-catalysis: K. Yamamoto, T. Shimizu, K. Igawa, K. Tomooka, G. Hirai, H. Suemune, K. Usui, *Sci. Rep.* **2016**, *6*, 36211.

[28] Center for Computational Research, University at Buffalo, http://hdl.handle.net/10477/79221.

Entry for the Table of Contents

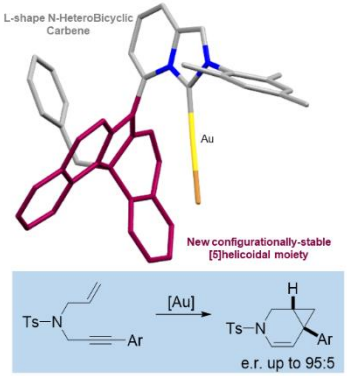

Helical-NHC ligands were for the first time used as chiral ligands in enantioselective gold(I) catalysis. The introduction of the chirality was realized in a key post-functionalization step and led to the generation of a chiral NHC laterally-substituted by a new configurationally-stable [5]-helicoidal moiety. This structural design allowed good activities and high ee values attained in gold-catalyzed cycloisomerization of N-tethered enynes.

Institute and/or researcher Twitter usernames: @vinc_cesar, @Bastin31, @JeanneCrassous, @LCC_CNRS, @chimie_ISCR